Library, L. M. A. L.

TECHNICAL MEMORANDUMS

NATIONAL ADVISORY COMMITTEE FOR AERONAUTICS

No. 865

BEHAVIOR OF STATIC PRESSURE HEADS AT HIGH SPEEDS

By Helmut Danielzig

Luftfahrtforschung
Vol. 14, No. 6, June 20, 1937
Verlag von R. Oldenbourg, München und Berlin

8.1
9.1.2
9.2
9.2.1

Washington
June 1938

NASA Technical Library
3 1176 01440 3472

NATIONAL ADVISORY COMMITTEE FOR AERONAUTICS

TECHNICAL MEMORANDUM NO. 865

BEHAVIOR OF STATIC PRESSURE HEADS AT HIGH SPEEDS*

By Helmut Danielzig

SUMMARY

The present report describes the development of a static pressure head for high speeds. The tests proved its practicability at speeds up to 400 km/h (248.5 m.p.h.). It weighs 6.5 kg or 2.5 times as much as the old head.

The position of the pressure head below the airplane was determined by bearing method at different speeds and for different lengths of suspension. It was established that for the measured speed range a 20 to 24 m suspension length was sufficient to assure a minimum distance of 6 m from the airplane without introducing any appreciable errors in the results due to wrong static pressure. A tubing for a speed of 600 km/h (372.8 m.p.h.) has been constructed as experimental project which, with a pressure head weighing 9 kg, should equally assure a sufficiently great vertical distance at this speed.

The supporting and pressure-tapping element is an all-metal tubing of 7 mm diameter and 4 mm inside width.

Parallel with the tests, a nomographic method was evolved for the rapid and accurate determination of the tubing curve. The practicability of the method is reflected by the comparative measurements and recommends itself also for the determination of airplane antenna curves.

I. INTRODUCTION

By virtue of its economical advantages and its remarkable precision, the pressure-head method is finding

---

*"Verhalten von statischen Sonden bei hohen Geschwindigkeiten." Luftfahrtforschung, vol. 14, no. 6, June 20, 1937, pp. 304-309.

widespread favor over the previously customary quadrangular flights for relative speed determinations and exact dynamic pressure calibrations. The pressure-head method is, as is known, based upon Bernoulli's fundamental equation:

$$p_{total} = p_{static} + p_{dynamic}$$

where the total pressure p_{total} is obtained with a DVL total-head meter and the static pressure p_{static}, by means of a static pressure head trailed several meters below the airplane. The two pressures yield as difference the true flight dynamic pressure. The conventional static pressure head heretofore used by the DVL weighs 2.4 kg while the tubing connecting with the airplane is a 20 m length of rubber hose of 8 mm outside and 3 mm inside diameter housed in wire netting. This instrument is not practical at speeds above 250 km/h, as the dynamic stability of the suspension cable becomes inferior at such speeds. The vibrations set up by gusts or irregularities in propeller slipstream no longer die out, but are propagated in direction of the hose end where the static pressure head itself is thrown into erratic oscillations of such amplitude that not only reading is falsified, but the airplane itself is endangered.

Another reason for not exceeding the cited speed of 250 km/h is that at higher speeds the head itself may be raised so high that it eventually finds itself in the wake of the airplane.

II. TEST PROCEDURE

In order to arrive at a satisfactory solution of the problem, the DVL made systematic flight tests with a Heinkel He 70. The floor plates were removed during these tests to provide an uninterrupted view of the pressure head and of the tubing. Above the two openings we mounted two bearing loops which, after sighting the pressure head on a sector scale, permitted the reading of the angle of the pressure head below the airplane with respect to a body-fixed reference axis (fig. 1). The distance of the bearing-loop axes amounted to 1.57 m. The measuring accuracy of the bearing device was close enough to remain

below a limit of error of ±0.5 m in the computation of the pressure-head position relative to the airplane. The static pressure tubing consisted of an all-metal hose of 7 mm outside diameter made by the Berlin-Karlsruher Industrie-Werke. The all-metal hose was preferred after previous tests had disclosed that the customary metal-wound rubber hose is occasionally squeezed off at the point of emergence from the airplane*. The total length of available hose was 24 m. The hose lead from a spool of 200 mm diameter over a roller to the pressure head. A dynamometer of 20 kg test range was provided to be installed in the hose portion between roller and spool and indicated the tension in the hose. Flight performance losses due to the drag component in flight direction were accounted for in measurements of the slope of the upper end of the hose relative to the longitudinal axis of the airplane. Agreement of the measurements with respect to time for the reading of the bearing-loop settings by two observers was insured by a light signal.

The flight tests were made at speeds of from 200 to 350 km/h. No readings were possible above this speed, because the pressure head was no longer within range of the forward bearing loop.

The speedometer employed in these flights was flight-tested over a square course. All measurements were made in horizontal flight as much as possible in order to preserve the condition of flow direction perpendicular to the direction of gravity. Compliance with this condition makes direct comparison of the free-flight data with the subsequently described calculation method for defining the tubing curve, possible. Horizontal flight was possible up to speeds of 330 km/h; increased to 350 km/h with full throttle, the airplane already exhibited a sinking speed of 2 m/s. Even so, the resulting errors remain within the bounds of measuring accuracy. In the first flight tests an experimental model consisting of a streamlined brass pipe of 40 mm diameter filled with hard lead and four plain fins was employed. The total weight of the model amounted to 5.4 kg. The same plain stabilizing fins were used on the final design (fig. 2) rather than the stabilizing cone with 3° angle of incidence (fig. 2a) used on the low-speed pressure head, which had proved impracticable for high speeds.

---

*Owing to the relatively short life of metal hose, various synthetic products are being investigated by the Institute for Aeronautics.

The pressure head was suspended, as already stated, from an all-metal tubing which at the same time served as supporting and pressure-tapping element. The point of suspension was provided directly above the center of gravity of the pressure head. A link connection between pressure head and tubing kept the lever arm and therewith the turning moment about the transverse axis of the pressure head to a minimum.

In the final version (fig. 2) the link consists of a sphere carried in the head and terminating at the top in a neck H 4 mm thick and 100 mm long. The upper end of H is hollow with a nipple N at the side. The neck is soldered to the metal tubing. A short piece of rubber hose serving as pressure tap, connects nipple N with the pressure-head nipple N_s, which in turn leads within the pressure head to the annular slot. A safety against turning of the spherical pivot about the normal axis of the pressure head prevents the rubber hose from becoming detached. Both the head and the stabilizing ring are of nickel-plated steel. The total length is 625 mm, for a diameter of D = 45 mm. The annular slot for tapping the static pressure lies 3 D aft of the foremost point of the pressure head. Wind-tunnel tests disclosed a 2.4 percent static-pressure difference as compared with the static reading of a calibrated Pitot tube of normal size.

III. RESULTS OF TESTS

Qualitatively, the flight tests revealed that both the pressure head and tubing remain so much more steady as the extensibility is less and the stability of the tubing greater, that is, the greater the restoring forces are which occur as soon as the tubing curve is changed by some outside influence, such as gusts, for instance. The stability of the tubing (apart from the cable stiffness which, however, is not attempted in the interest of windability), is chiefly influenced by the weight of the instrument. It was noticed that all oscillatory motions set up during the measurements originated in the upper part of the tubing exposed to propeller slipstream and wing wake, while the head itself was only indirectly set in vibration. These vibrations are at right angles to the direction of flight. By increasing the weight from 2.4 kg (weight of the old pressure head) to 5.4 kg (weight of experimental model)

and employing the cited metal tubing, it was possible to lower these transverse oscillations to a minimum. This arrangement damps out even oscillations set up in gusty weather remarkably quickly without causing any appreciable disturbance of the head itself.

Having succeeded in the matter of weight of pressure head and type of tubing to insure in principle perfect performance up to speeds of almost 400 km/h the position of the pressure head with respect to the airplane was determined at speeds of from 210 km/h to 350 km/h with tubing of 12, 16, 20, and 24 m length.

With the notation of figure 1, the depth and trail of the pressure head follow from the relations:

$$z = a \frac{\sin k_1 \sin k_2}{\sin (k_1 - k_2)} \text{ [m]} \tag{1}$$

$$x = a \frac{\cos k_1 \sin k_2}{\sin (k_1 - k_2)} \text{ [m]} \tag{2}$$

Figure 3 shows the depth z from the measuring base a parallel to the longitudinal airplane axis plotted against the speed, with tubing length as parameter. With tubing of 20 m length, the normal depth 9.7 m drops to 6.5 m when the speed changes from 210 to 350 km/h, which, extrapolated to 400 km/h, still leaves a depth of 6.0 m. This length should undoubtedly suffice to reduce the error in reading resulting from the falsification of the static pressure to a practically insignificant magnitude (reference 1).

The effect of the suspension length on the normal distance from the reference base is comparatively small within the explored limits according to figure 3. Doubling the length from 12 to 24 m increases, at 300 km/h, the distance from 5.5 to 7 m, i.e., a 100-percent-length change produces only a 27 percent change in depth. With greater hose lengths the change becomes even less, because the angle of exit of the hose from the airplane becomes consistently less on account of the greater total drag.

Much more important is the influence of the suspension length upon the position of the head behind the airplane.

Lengthening the hose from 12 to 24 m results in more than twice as great a change in trail, according to figure 4. Within the measured interval, both the depth and trail of the head change approximately linearly with the speed.

In order to assess the speed losses due to the head and the suspension tube, the force and direction of the suspension tube on the airplane body must be known. Figure 5 depicts these quantities for a 16 m suspension length against the flying speed. The greatest force recorded on the tubing amounts to ~10 kg. The two quantities give the force component in flight direction. It is advised to use the static pressure head, especially on smaller airplanes, only for calibrating the recording instruments, but to make the tests themselves with reeled-in head. With known airplane quantities the corresponding proportionate ΔC_w and thence with available airplane polar the following relation is obtained:

$$\frac{V_{Fl\ +\ \text{air-speed head}}}{V_{Fl}} = \sqrt[3]{\frac{c_w}{c_w + \Delta c_w}} \qquad (3)$$

whereby:

$V_{Fl\ +\ \text{air-speed head}}$ = flying speed with air-speed head,

V_{Fl} = flying speed without air-speed head,

c_w = drag coefficient of airplane,

Δc_w = drag coefficient of air-speed assembly.

This holds for horizontal flight, i.e., thrust = drag.

IV. DESCRIPTION OF NOMOGRAPHIC METHOD EMPLOYED TO DEFINE THE SUSPENSION-HOSE CURVE

There are several known methods of defining the form of the curve resulting from towing heavy bodies from a flexible cable through air for the purpose of predicting the position of the air-speed head in space. However, these methods are in part time-consuming, or, as is the case of Glauert's method (reference 2), they proceed from assumptions regarding the lift and drag of the hose, which are considerably at variance with corresponding wind-tunnel tests. For this reason, it seemed expedient to evolve a method which conformed to actual conditions over a wide field, as well as being short. And the results as regards desirable accuracy fulfilled our expectations.

The method is predicated on a chord curve rather than the sag curve and postulates that the cable stiffness of the suspension has only a minor influence on the form of the curve itself owing to the comparatively great curvature radii of the curve.

The suspension hose is first divided into chord pieces of equal finite length. Chord lengths of 50 cm proved small enough to be serviceable as substitute for the related arc piece as theoretical basis.

Notation

c_a, lift coefficient of a hose element

c_w, drag coefficient of a hose element

q, flight dynamic pressure (kg/m²)

$A_{1,2}$ vertical force component at hose element (kg)

$B_{1,2}$ horizontal force component at hose element (kg)

Δl length of suspension hose element (m)

d diameter of suspension hose (m)

$\Delta F = \Delta l d$ area of suspension hose element (m²)

G_s, weight of suspension hose element (kg)

α_s, angle of incidence of a suspension-hose element to the flow (deg.)

A_s, lift of a suspension-hose element (kg)

W_s, drag of a suspension-hose element (kg)

G, weight of air-speed head (kg)

W, drag of air-speed head (kg)

Figures 6 and 7 depict the lift and drag for metal-wound suspension hose of 7 and 8 mm diameter, respectively. The angle of incidence of the suspension hose ranges between 15 and 75 under practical conditions. A good approximation is:

$$c_w = C \sin^2 \alpha_s \tag{4}$$

$$c_a = C_1 \sin^2 \alpha_s \cos \alpha_s \tag{5}$$

It involves empirically defined functions whose validity for different tube diameters was confirmed in wind-tunnel tests of the DVL. On these premises, the average error remains considerably below 10 percent in contrast to the 30 percent by Glauert's method.

With (4) and (5), the lift and drag of a chord element are:

$$\left.\begin{aligned} W_s &= q\ \Delta F\ C \sin^2 \alpha_s \\ \underline{W_s} &\underline{= C_2 \sin^2 \alpha_s} \end{aligned}\right\} \tag{6}$$

$$\left.\begin{aligned} A_s &= q\ \Delta F\ C_1 \sin^2 \alpha_s \cos \alpha \\ \underline{A_s} &\underline{= C_3 \sin^2 \alpha_s \cos \alpha_s} \end{aligned}\right\} \tag{7}$$

whence figure 8, in conjunction with the equilibrium conditions for a hose element, gives:

$$\Sigma V = 0 : A_n + C_3 \sin^2 \alpha_s \cos \alpha_s - G_s - A_{n-1} = 0 \tag{8}$$

$$\Sigma H = 0 : B_n - B_{n-1} - C_2 \sin^2 \alpha_s = 0 \tag{9}$$

$$\Sigma M = 0 : A_{n-1} \Delta l \cos \alpha_s + G_s \frac{\Delta}{2} \cos \alpha_s - B_{n-1} \Delta l$$

$$\times \sin \alpha_s - W_s \frac{\Delta l}{2} \sin \alpha_s - A_s \frac{\Delta l}{2} \cos \alpha_s = 0 \qquad (10)$$

The introduction of the functions for A_s and W_s and division by

$$\frac{C_3 \Delta l \sin \alpha_s}{2}$$

in equation (10) gives

$$\frac{2 A_{n-1}}{C_3} \cot \alpha_s + \frac{G_s}{C_3} \cot \alpha_s - \frac{2 B_{n-1}}{C_3}$$

$$- \frac{C_2}{C_3} \sin^2 \alpha_s - \sin \alpha_s \cos^2 \alpha_s = 0 \qquad (11)$$

or

$$\sin \alpha_s \cos^2 \alpha_s + \frac{C_2}{C_3} \sin^2 \alpha_s + \frac{2 B_{n-1}}{C_3} = \frac{2 A_{n-1} + G_s}{C_3} \cot \alpha_s \qquad (12)$$

For the tip of the head, it is $A_{n-1} = G$ and $B_{n-1} = W$; W must be ascertained in the wind tunnel.

Equation (11) combined with (8) and (9) could already be used as recursion formula. But the purely analytical solution for a function of α_s is so difficult that the nomographic method of solution was preferred.

The nomograph is essentially a system of two scales (fig. 9). The left-hand scale is vertically graduated for the cot function, that is, for different coefficients $\frac{2 A + G_s}{C_3}$ which are of the anticipated order of magnitude of the coefficient of $\cot \alpha_s$ in equation (11). Figure 9a, containing the function,

$$A = f\left(\frac{2 A + G_s}{C_3}\right)$$

facilitates the finding of the coefficients relevant to the different A.

The right-hand scale in figure 9, containing the other three terms of (12), is in two parts. The part above the traced abscissa comprises the sum of the two terms to the left of the equals sign

$$\sin \alpha_s \cos^2 \alpha_s + \frac{C_2}{C_3} \sin^2 \alpha_s$$

While the cited upper part of the ordinate depends, apart from α_s, only on the ratio $\frac{C_2}{C_3} = \frac{C}{C_1}$ i.e., on the ratio of the coefficients of lift and drag and consequently assumes other values simply as form factor for different tubings, the lower part carries the function $\frac{2\ B}{C_3} = f(B)$. The different straights correspond to different C_3, i.e., different impact pressures for chosen thickness and length of the tubing elements.

Figures 10 and 11 facilitate the determination of forces A_n and B_n in (8) and (9). They render the tracing of $C_2 \sin^2 \alpha_s$ and $C_3 \sin^2 \alpha_s \cos \alpha_s$ for different α_s and C values, possible.

First, the constants C and C_1 are ascertained from the wind-tunnel curves (equations (4) and (5)). Then, the choice of chord length, tubing diameter, and impact pressure is followed by the calculation of:

$$C_2 = \Delta\ l\ d\ q\ C \tag{13}$$

$$C_3 = \Delta\ l\ d\ q\ C_1 \tag{14}$$

As the construction of the tubing curve starts from the free end of the suspension tubing, the drag and weight of the air-speed head must be established first.

Then the chord curve is built up with the above quantities as follows:

1) Determine value $\frac{2\,A + G_s}{C_3}$ from figure 9a (for start $A_{n-1} = G$) and ascertain in figure 9.

2) Determine $\frac{2\,B_{n-1}}{C_3}$ in figure 9 (for start $B_{n-1} = W$).

3) Connect both points and shift parallel upward, until equal angles appear on the ordinates (plot the 1st chord element).

4) Define the new A from the preceding A by subtracting G_s and adding the amount of lift which corresponds to the just found α_s in figure 11.

5) Determine the new B from the previous B, by adding the amount of the drag which corresponds to the just found α_s in figure 10.

6) Proceed with A and B as under 1, 2, 3.

Concerning point 3, it should be noted that the parallel shift merely fulfills the condition (equation 12), which postulates that the sum of the terms on the left-hand side of the equation is equal to the term on the right-hand side.

The tubing curves I, II, III in figure 12 were obtained by this method. Curves I and III are for the heavy air-speed head at 210 and 350 km/h, while curve II indicates the position of the small air-speed head at 210 km/h.

The dots designating the various speeds on which the calculation was based, are actual positions of the air-speed head in space as measured by bearing in flight. The comparison of the measured and the computed values manifests ample agreement.

Curve IV in figure 12, also established by nomographic method, is for a flying speed of 600 km/h and 25 m suspension length for an air-speed head of 9 kg.

Translation by J. Vanier,
National Advisory Committee
for Aeronautics.

REFERENCES

1. Kiel, Georg: Fehlerabschätzung bei Standruckeichungen mittels unter dem Flugzeug geschleppter Sonden. Luftfahrtforschung, vol. 14, no. 6, June 20, 1937, pp. 310-313.

2. Glauert, H.: Heavy Flexible Cable for Towing a Heavy Body Below an Aeroplane. R. & M. No. 1592, British A.R.C., 1934.

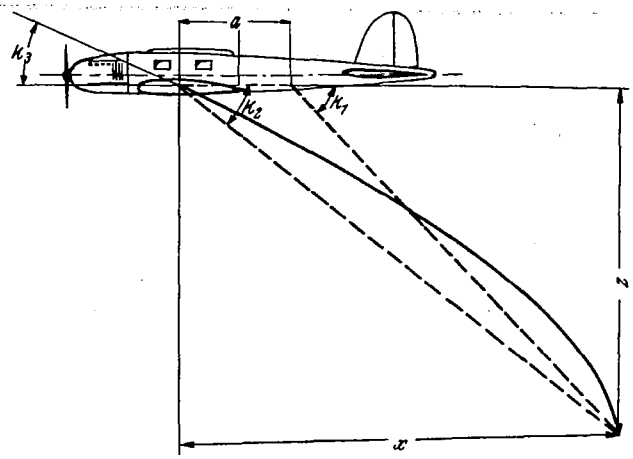

Figure 1.- Heinkel He 70 with static pressure head for high speeds (up to 400 km/h.). Experimental arrangement for ascertaining the depth and trail.

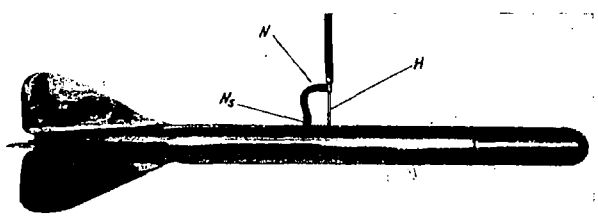

Figure 2.- Static pressure head for high speeds; total length; 625 mm; weight 6.5 kg; range up to 400 km/h; tubing diameter: 7 mm; H: thrust; N=nipple, N_s= pressure head nipple.

Figure 2a.- Low-speed pressure head; total length: 450 mm; weight: 2.4 kg; range; to 250 km/h.

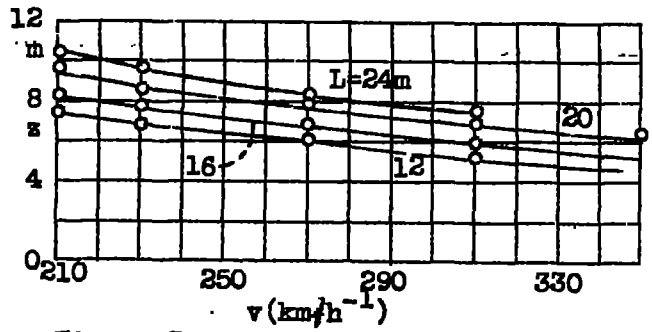

Figure 3.- Relation of depth to flying speed with different suspension lengths.

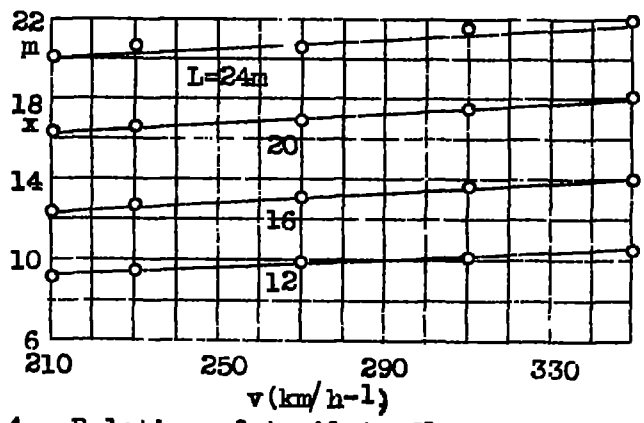

Figure 4.- Relation of trail to flying speed with different suspension lengths.

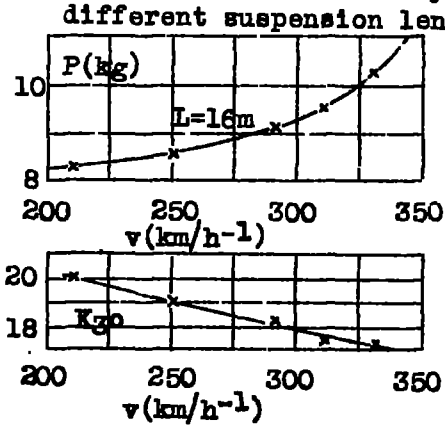

Figure 5.- Tensile stress P and direction K_3 of suspension tubing at airplane body against flying speed with 16 m suspension length.

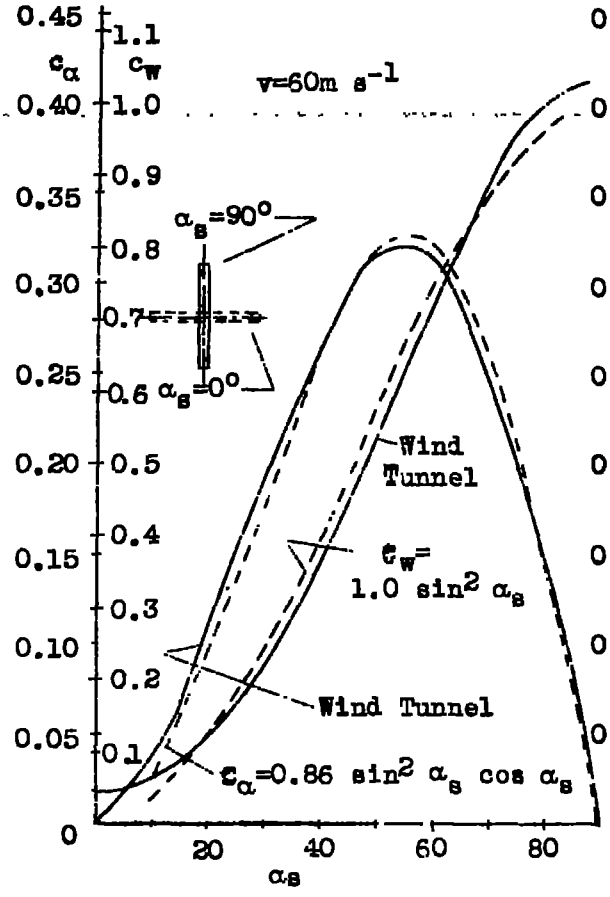

Figure 6.- 7 mm diameter.

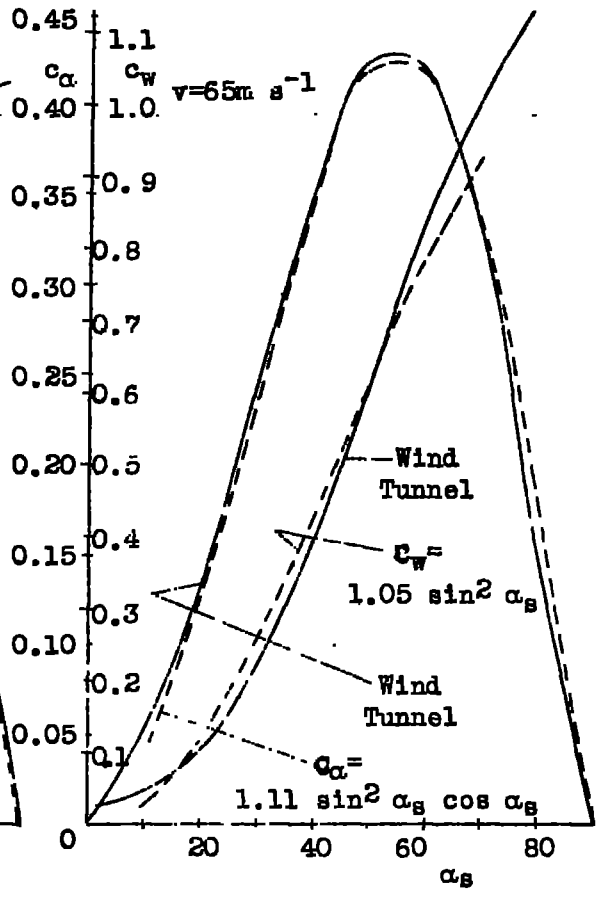

Figure 7.- 8 mm diameter.

Relation of lift and drag coefficients to angle of incidence for suspension tube element of 400 mm length.

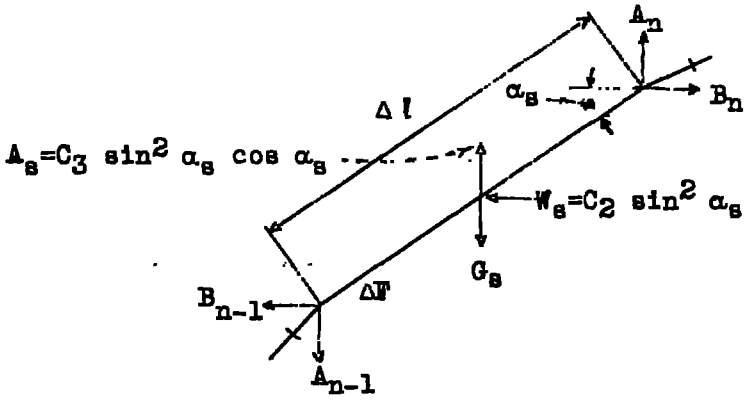

Figure 8.- Force distribution on an element of the suspension tubing.

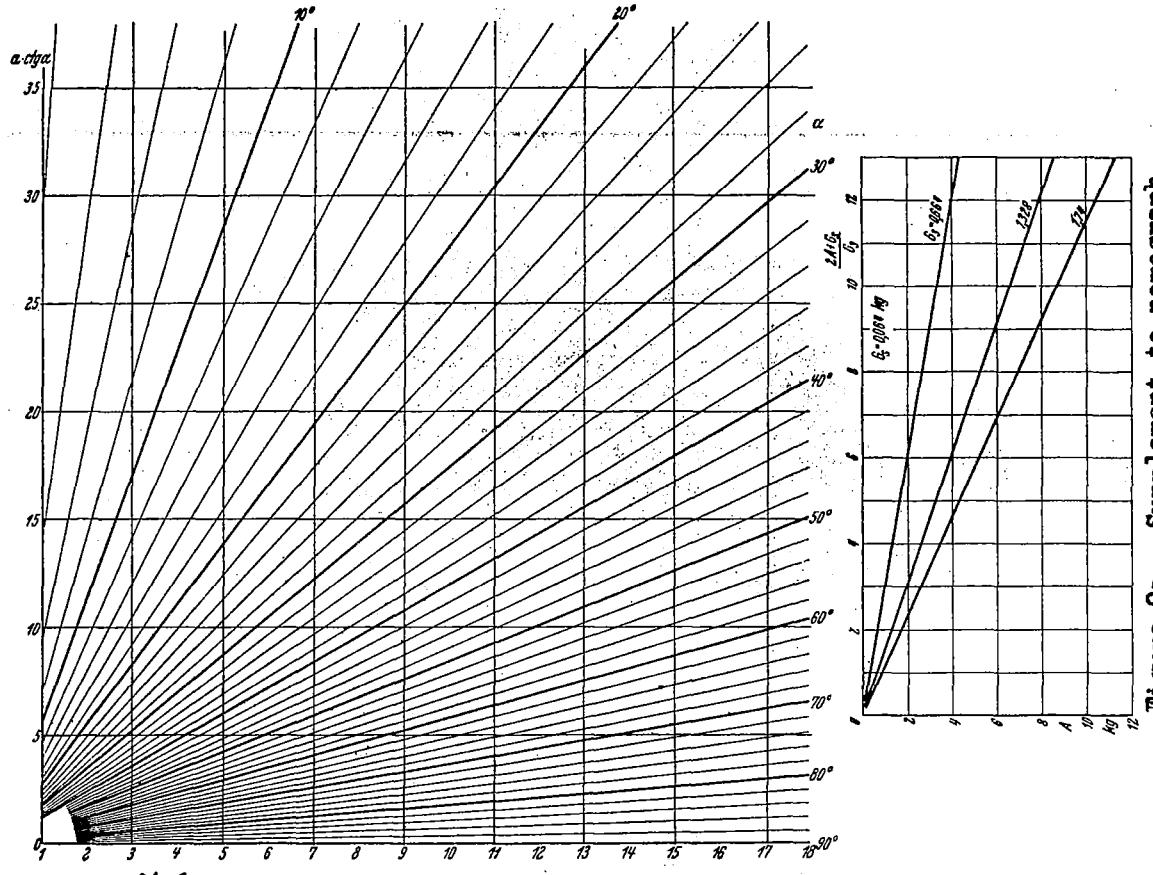

Figure 9a.- Supplement to nomograph.

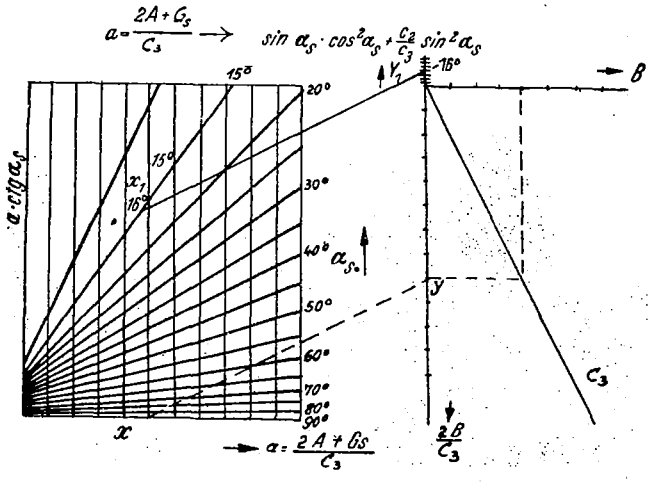

Explanatory sketch to the nomographic method: (see Fig. 9): after finding points x and y the relevant intersecting straight is shifted parallel until the ordinates, for example, at x_1 and Y_1 disclose equal angles.

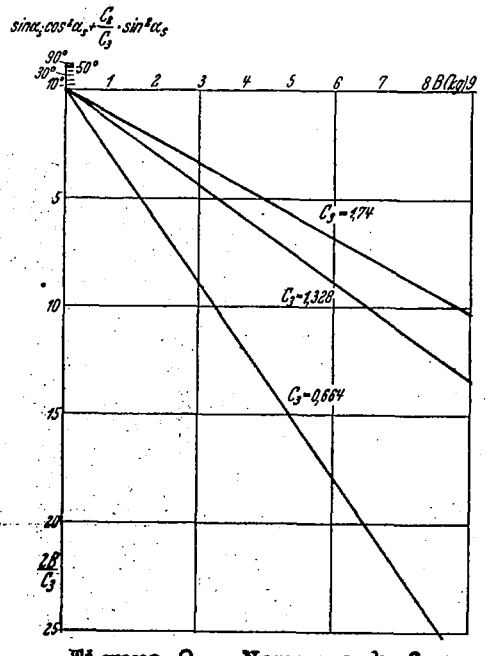

Figure 9.- Nomograph for obtaining the suspension tube curve.

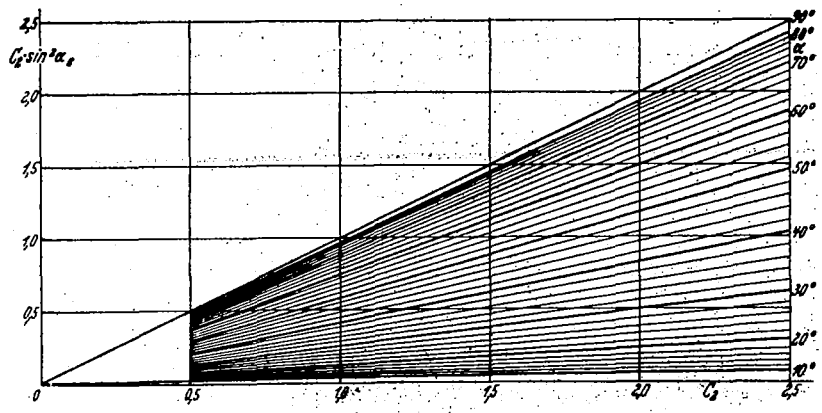

Figure 10.- Graph for defining the drag of a suspension tube element at different C_2 and α_s

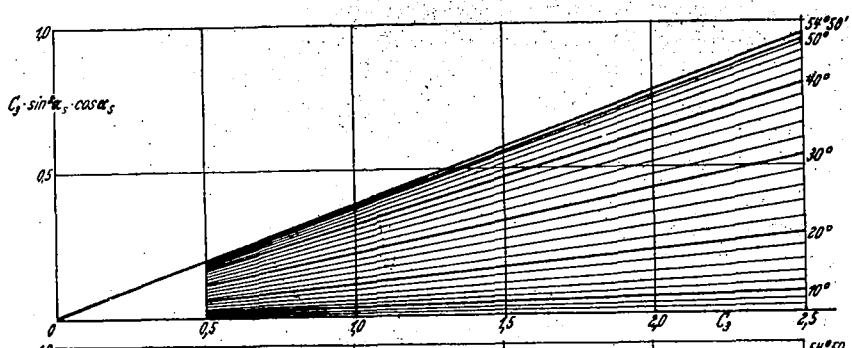

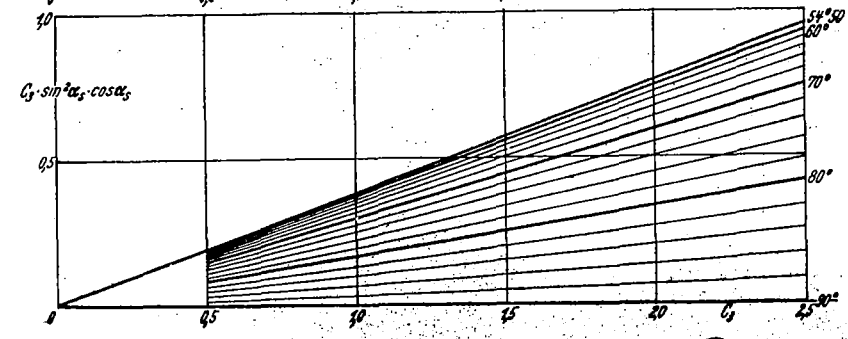

Figure 11.- Graph for obtaining the lift of a suspension tube element at different C_3 and α_s

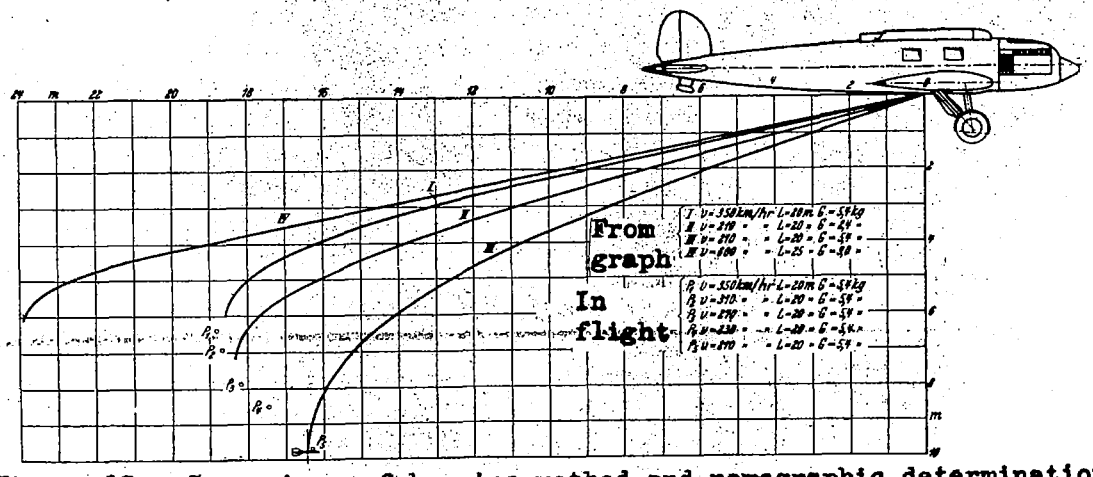

Figure 12.- Comparison of bearing method and nomographic determination of the position of the air speed head with respect to the airplane at different speeds.

NASA Technical Library
3 1176 01440 3472